A R C H I V E S O F M E T A L L U R G Y A N D M A T E R I A L S
Volume 53 2008 Issue 3

B. KUŹNICKA*, M. PODREZ-RADZISZEWSKA*

# CORRELATION BETWEEN MICROSTRUCTURAL EVOLUTION IN HEAT AFFECTED ZONE AND CORROSION BEHAVIOUR OF AL-CU ALLOY

# ZALEŻNOŚĆ MIĘDZY ZMIANAMI MIKROSTRUKTURY W STREFIE WPŁYWU CIEPŁA A PRZEBIEGIEM KOROZJI STOPU UKŁADU AL-CU

The purpose of this work was to investigate microstructure of a heat affected zone (HAZ) of aluminium alloy 2017A-T4 to determine its effect on corrosion behaviour of this alloy. The microstructure in HAZ was simulated by local rapid heating of the alloy and immediate cooling in air. Corrosion testing was performed by exposure to marine onshore atmosphere. The microstructure examinations were carried out using light microscopy, scanning electron microscopy, X-ray energy dispersion and X-ray diffraction analysis. A clear correlation was found between microstructure and susceptibility to intercrystalline and pitting corrosion in the zones heated to temperatures below, close and above the solvus line.
*Keywords*: aluminium; intermetallic; SEM, intergranular corrosion, pitting corrosion

Celem pracy było zbadanie zmian mikrostruktury w strefie wpływu ciepła (SWC) stopu 2017A-T4 oraz określenie jej wpływu na przebieg korozji stopu. Zmiany mikrostruktury analogiczne do zmian w SWC połączeń spawanych otrzymano przez lokalne, szybkie nagrzanie jednego końca rurowej próbki i natychmiastowe ochłodzenie w powietrzu. Badania korozyjne przeprowadzono poddając stop ekspozycji w atmosferze klimatu morskiego, w głębi lądu. Badania mikrostruktury przeprowadzono przy zastosowaniu technik mikroskopii świetlnej, elektronowej mikroskopii skaningowej, analizy dyspersji energii promieniowania rentgenowskiego oraz analizy dyfrakcji rentgenowskiej. Znaleziono wyraźną korelację pomiędzy mikrostrukturą a podatnością stopu na korozję międzykrystaliczną i wżerową w strefach nagrzania do temperatury niższej, bliskiej i wyższej od linii granicznej rozpuszczalności.

## 1. Introduction

Wrought age-hardenable 2xxx series alloys are used in architecture, automotive, machine building and aerospace applications because of their favourable strength-to-weight ratio. A disadvantage of this alloy group is jest susceptibility to different forms of corrosion like pitting corrosion, intergranular corrosion or exfoliation corrosion, especially in chloride-containing environments. Susceptibility to intergranular corrosion and to other localized corrosion forms depends on distribution of second phase precipitates rich in copper, which act as cathodic sites in relation to the surrounding solid solution matrix. Shape, size and distribution of the second phase precipitates are determined by the processing route (homogenization and ageing parameters, forming, welding or surface laser melting) carried out on the aluminium alloy.

Many research works [1-4] were devoted to examining the microstructural mechanism underlying the ageing processes in the alloys based on Al-Cu system using newly developed techniques. It is suggested that the precipitation sequence in this system contain one or more of the following processes:

supersaturated solid solution (sss)← GP zones → $\theta''$ → $\theta'$ → stable $\theta$

or, according to a modified interpretation of the precipitation process [2]:

sss → quenched clusters → GP(I)→ GP(II)→ $\theta''$ (independent of GP(II)) → $\theta'$ → $\theta$.

In the modified interpretation, the metastable phases are differentiated and their new terminology suggested: monolayer copper platelet (quenched clusters and slightly larger GP(I)), bilayer structures (GP(II)) and multilayer structure ($\theta''$), so that each precipitation stage corresponded to the stage observed on the hardness curve.

The complete precipitation sequence can only occur during isothermal ageing at the temperatures below the GP zone solvus (Fig.1). During isothermal ageing, transformation of one phase to another occurs by het-

* INSTITUTE OF MATERIALS SCIENCE AND APPLIED MECHANICS, WROCŁAW UNIVERSITY OF TECHNOLOGY, 50-370 WROCŁAW, POLAND

erogeneous nucleation at the sites of the previous phase, resulting in fine and uniform precipitates. However, it is easy to predict, looking at Fig. 1, that in the conditions of rapid heating above the solvus line (which happen e.g. in a heat affected zone during welding or surface laser melting), the processes of dissolution and formation of individual phases starts at higher temperatures, proceeds faster and can lead to detrimental changes of composition and morphology of the precipitates in comparison to isothermal ageing [5-7]. This undoubtedly affects both mechanical properties of the Al-Cu system alloys and their corrosion resistance. It should be also considered that the phase composition of multicomponent industrial alloys is different from the model alloys because of the presence of coarse intermetallic phases particles which impact on corrosion resistance can not be omitted.

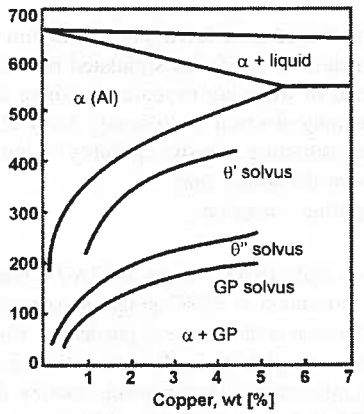


Fig. 1. Al-Cu phase diagram. Metastable solvus limits for GP zones, $\theta''$ and $\theta'$ phases and the equilibrium solvus line for the $\theta$ phase. After Ringer [1]

According to the research works [8-12] on corrosion resistance of this group of alloys in an environment containing chlorine ions, pitting and exfoliation are caused by non-uniform distribution of second phase particles resulting in forming a galvanic coupling with the matrix. Electrochemical mechanism for intergranular corrosion of Al-Cu alloys is often based on existence preferential anodic path along grain boundaries [13-15]. This active region along grain boundaries is thought to be caused by either solute depleted zones or anodic precipitates. This electrochemical framework was used to explained IGC in Al-Cu and Al-Cu-Mg alloys. It was proved that IGC is not due to a difference in potentials between grain boundaries and grain bodies but to a difference in breakdown potentials of those phases. This occurs when, as a result of ageing, a Cu-depleted zone is created along the grain boundaries with the potential lower than that of the grain bodies.

In this study, corrosion behaviour of the 2017A-T4 alloy was investigated in a marine onshore atmosphere. The purpose of this work was to explain the susceptibility of the alloy towards intergranular and pitting corrosion introduced by local rapid heating one of the ends of the tubular specimen to temperature below the solidus line and to find correlation between the microstructure evaluated in heat affected zone (simulated this way) and the form of corrosion.

## 2. Experiments

The examinations were carried out on a tube section 0.6 m long. It was a single commercial extruded tube sized 65 mm (OD) × 4 mm (WT), grade EN AW-2017A-T4 acc. to EN 573. Chemical analysis of chips taken from the tube was made by the gravimetric method. The results are given in Table 1. Hardness measurements were taken on the tube surface, by Vickers method at 9.807 N acc. to EN ISO 6507. The obtained values of (214 ± 4) HV1 indicated the condition after natural ageing, corresponding with T4 temper acc. to EN 515.

To simulate the microstructure developed in HAZ of aluminium alloy welds, one of the tube ends was induction heated to ca. 555 °C (above the eutectic temperature of 547 °C and below the solidus line, as can be seen in Fig.1). This enabled obtaining a temperature gradient determining the processes of precipitating and dissolution of the secondary phases with no liquation phenomena of the grain boundaries. Changes in microstructure were preliminarily detected by determining hardness distribution on the tube length (see Fig. 2), on which ground the places of taking samples for microscopic examinations were traced out.

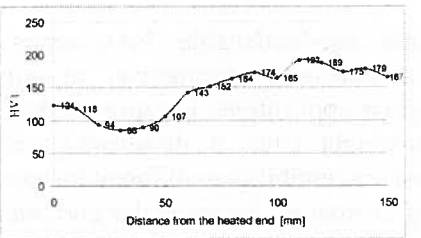


Fig. 2. Vickers hardness in heat affected zone of tubular specimen of 2017A-T4 alloy heated at one end and cooled in air

Corrosion testing was performed on the specimen by exposing it to service environment, i.e. the marine onshore atmosphere. The susceptibility to corrosion was determined by metallographic examination of the specimens after outdoor exposure for 4 years. On the ground of appearance of the inside tube surface after exposition (see Fig. 3) and the determined hardness distribution (Fig. 2) the specimens for microscopic examination were cut out at the distances of 0, 10, 30, 60 and 110 mm from the face of heated tube end.

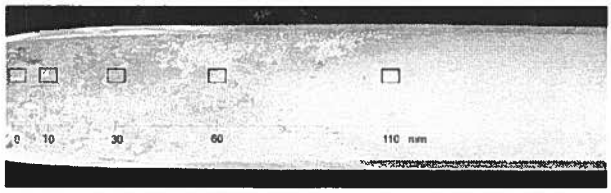


Fig. 3. Corrosion marks on inside surface of a tube section of 2017A-T4 alloy one-end heated to ca. 555 °C after 4-year exposure in marine onshore atmosphere. Places of cutting-out of specimens

Characterisation of microstructure was performed by an optical microscope, a Jeol-JSM 5800 LV scanning electron microscope (SEM) equipped with EDX analysis system and a Siemens D500 X-ray diffractometer (XRD). Microscopic examination was carried out on longitudinal radial and tangent sections, unetched and etched with the solution of 0.5 ml HF (40 %) in 99.5 ml of distilled water.

## 3. Results and discussion

The as-delivered 2017A-T4 alloy contained coarse second phase particles distributed in $\alpha$-Al matrix (Fig. 4). The particles were moderately aligned with the direction of hot extrusion. Some of them were arranged on grain boundaries. Results of SEM/EDX and XRD analysis showed that they were mainly round-shaped $\theta$-$Al_2Cu$ particles and irregularly or shell-shaped particles (black-coloured particles in Fig. 4), mainly of Al-Cu-Mn-Fe-Si. Cathodic nature of the Al-Cu-Mn-Fe-Si particles in relation to the matrix was confirmed by several authors [8,16]. Grains of $\alpha$ solid solution were elongated in both the longitudinal and circumferential directions and flattened in the radial direction.

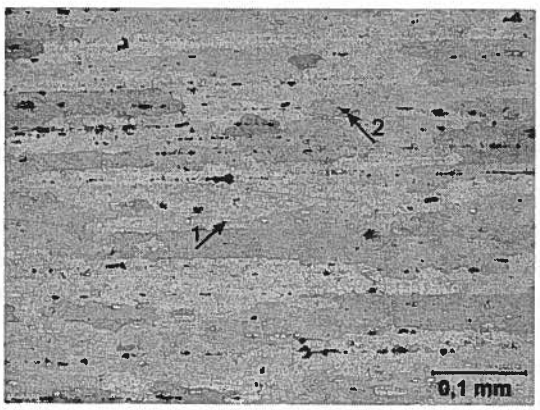


Fig. 4. Coarse intermetallic particles in naturally aged 2017A alloy: 1 – $\theta$-$Al_2Cu$ particles, 2 – Al-Cu-Mn-Fe-Si-containing particles. Longitudinal section, etched

After 4-year exposure in the marine onshore atmosphere, the examined tube section suffered corrosion, but in the heat affected zone only. On the outer surface, corrosion marks occurred on the distance of ca. 20 mm from the heated tube face. On the inner surface however, due to the conditions favourable for longer moisture staying, corrosion covered the area reaching 120 mm, see Fig. 3.

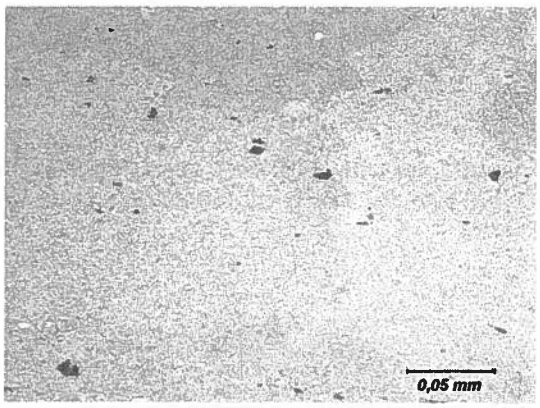


Fig. 5. Microstructure in HAZ of 2017A alloy at 110 mm from the face of heated tube end. Uniform distribution of dispersed particles. Longitudinal section, etched

It was found that, as could be expected, the alloy was subject to overageing in the heated zone. Extent of this zone corresponds approximately to the extent of the surface corrosion marks. At the distance of 80 to 120 mm from the heated tube end, rapid heating caused heterogeneous nucleation of $\theta$ phase at the sites of earlier products (GP zones or $\theta'$, $\theta''$) resulting in fine and uniformly dispersed precipitates, with no precipitate-free zone along grain boundaries (Fig. 5). This is the reason for a slight hardness drop in this zone, as compared to the initial condition. At the distance of 30 to 80 mm, a clear hardness drop can result only from growth of the precipitates, because their uniform distribution was maintained. At the distance of ca. 10 to 20 mm, a clear, bright line of grain boundaries appears, see Fig. 6. This results from heating the alloy above the solvus line, as evidenced by the visible in Fig. 7 initial stage of the large $\theta$ particles dissolution and the surrounding particles precipitation-free zone. Precipitates on grain boundaries, bright boundary line between the precipitates and precipitation-free zone along grain boundaries can be indicative for diffusion of copper to the grain boundaries during cooling. However, linear qualitative analysis by EDX did not show any drop of copper concentration in the precipitate-free zone. A slight hardness increase (Fig. 2) can be attributed to the process of precipitation of dispersive phases from partially supersaturated solid solution due to the subsequent natural ageing.

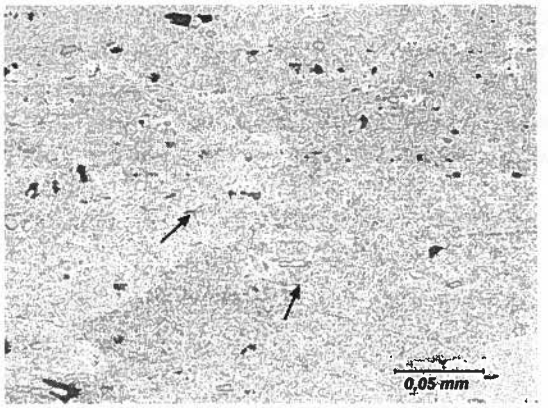


Fig. 6. Microstructure in HAZ of 2017A alloy at 10-20 mm from the face of heated tube end. Grain boundary precipitates. Longitudinal section, etched

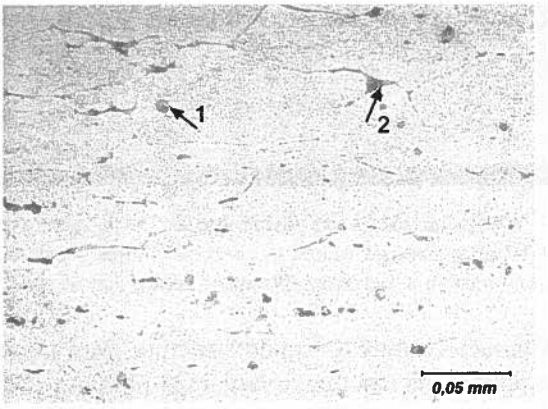


Fig. 8. Microstructure in HAZ of 2017A alloy at <10 mm from the face of heated tube end. Non-equilibrium melting: 1 – eutectic colonies, 2 – degenerated eutectic colonies. Longitudinal section, etched

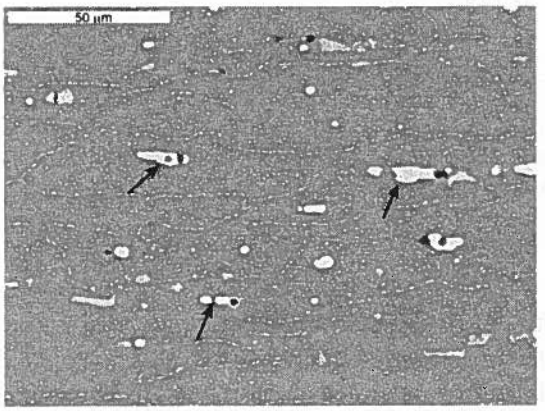


Fig. 7. SEM micrograph of microstructure shown in Fig. 7. Visible initial stage of coarse particles dissolution (arrows) and grain boundary precipitates

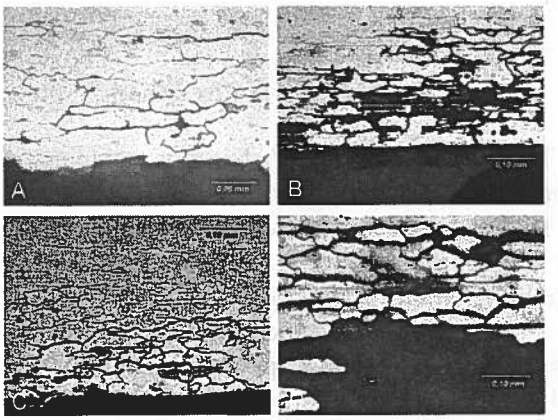


Fig. 9. Corrosion attack for 2017A alloy after 4-year exposure in marine atmosphere: a – distance from the face ca. 110 mm, intergranular corrosion; b – distance from the face 60 - 70 mm, intergranular corrosion plus tunnel-like pitting; c – distance from the face 10 - 20 mm, intergranular corrosion plus pitting; d – distance from the face less than 10 mm, intergranular corrosion. Longitudinal sections, etched

Near the heated end, the phenomenon of non-equilibrium melting occurred as a result of rapid heating above the eutectic temperature of 548 °C and immediate cooling [17,18]. Melting started at the interface between coarse $\theta$ particles and the matrix. Liquid created droplets inside the grains and spread along grain boundaries. Because of immediate cooling it solidified forming fine eutectic rosettes inside the grains and particles of regular or degenerate eutectic along grain boundaries (Fig. 8). Particles of the phase Al-Cu-Mn-Si-Fe remained undissolved. The precipitation-free, bright areas visible in Fig. 8 indicate that during heating a significant part of the small particles dissolved in the solid solution. This means also that, after cooling and as a result of natural ageing, there are coexisting coarse particles of $\theta$ phase as components of the regular or degenerated eutectic at grain boundaries, dispersed precipitates inside the grains (visible in Fig. 8) and invisible coherent or semi-coherent $\theta''$ or $\theta'$ precipitates. This explains hardness increase from 86 HV1 to 124 HV1 (Fig. 2) as approaching to the heated tube end, starting from the distance of 30 mm.

Corrosion in the longitudinal sections shown in Figs 9a-d indicates that intergranular corrosion and pitting corrosion occurred in the heat affected zone. IGC dominates to the degree dependent on the heating temperature, first of all on its relation to the solvus or eutectic temperature. In the zone heated to the temperature not exceeding the solvus line, along with increasing overageing degree the attack on the grain boundaries was stronger and the subsequent corrosion of the whole grains was more intensive (Figs. 9 a,b). Beyond the heated zone (naturally aged condition), the material proved to be corrosion resistant. Such a corrosion behaviour seems to be consistent with the theory stating that IGC of aluminium alloys results from microgalvanic cell action at the grain boundaries, related to grain boundary precipitates which are more noble than the surrounding matrix of aluminium-based solid solution [10,13,14]. The consequence of rapid heating with subsequent air-cooling

is the diffusion-controlled precipitation and growth of copper-containing precipitates on grain boundaries resulting finally in depletion in copper at grain boundaries. The lower heating temperature, the narrower is the copper-depleted zone and narrower corroded grain path. However, the SEM observation and EDX analysis of the grain boundaries did not reveal any depletion in copper in comparison with the grain interior. At higher temperatures, copper concentration in the matrix and along the grain boundaries becomes equalized and corrosion of grain bodies begins (Fig. 9b). The attack on the grain bodies takes the form of tunnels, similar to the ones observed by Galvel for binary Al-Cu alloys [13].

In the zone heated above the solvus line it is difficult to evaluate the distribution of copper concentration in the matrix and the boundary zones, because short heating time does not permit complete dissolution of the hardening phases and air-cooling enables diffusion of copper to the grain boundaries. In the zone heated to a temperature not exceeding the eutectic temperature, the intergranular corrosion was dominating, although the bodies of some grains showed pitting (Figs. 9c, 10). As can be seen in Fig. 10, intergranular corrosion seems to be a result of dissolving the matrix around the chain-arranged precipitates along the grain boundaries. The EDX analysis of the precipitates inhered in the dissolved boundaries evidenced that they are particles of $\theta$ phase (mainly) and the phase Al-Cu-Mn-Fe-Si. It can be also seen that, because of dissolving the surrounding matrix around the coarse particles, a lot of them fell out.

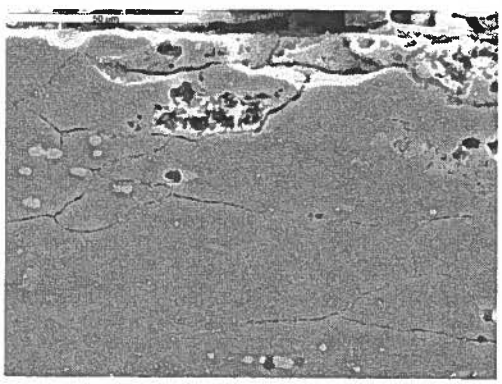

Fig. 10. Magnified detail of Fig. 9c. SEM

In the zone heated above the eutectic temperature, strong intergranular corrosion occurred. This can be caused by lower copper concentration in the precipitation-free zones around the eutectic colonies, which form an almost continuous network along the grain boundaries. IGC was intensified by increased copper concentration in the matrix inside the grains due to dissolution of significant quantity of dispersed and coarse particles during heating. Increasing Cu concentration in $\alpha$-matrix reduced susceptibility of the grain bodies to pitting corrosion [9,10]. However, linear EDX analysis through the eutectic colonies did not reveal lower copper concentration in the precipitation-free zone with respect to the remaining matrix, but showed a depletion of silicon (Fig. 11). Depletion of silicon can have an influence on the areas surrounding the particles making them active and susceptible to corrosion by microgalvanic action. This suggests that researches on the corrosion mechanism of aged industrial alloys series 2xxx should consider the influence of the alloying elements dissolved in a part in the solid solution and in a part in the intermetallic phases.

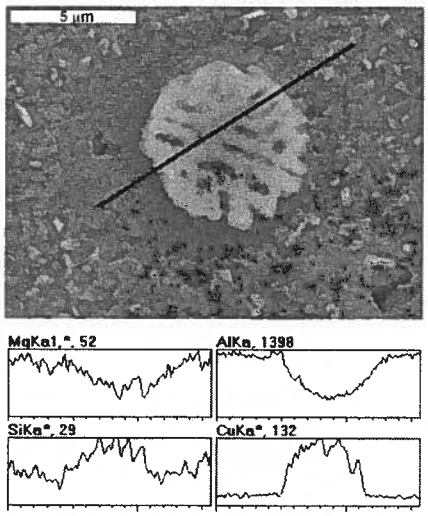


Fig. 11. Linear EDX analysis across an eutectic colony

## 4. Conclusions

1. The aluminium alloy 2017A in naturally aged condition is resistant to corrosion in marine onshore atmosphere, however overageing affects its corrosion susceptibility to the degree dependent on the heating temperature.
2. Forms of the corrosion attack in heat affected zone are determined by the heating temperature in comparison to the solvus line:
   - Rapid heating to a temperature below the solvus line intensifies the overageing process and causes IGC. In the zone heated to a temperature close to the solvus line, IGC is accompanied by tunnel-like pitting.
   - Rapid heating to a temperature above the solvus line causes dissolution of hardening phases and coarse particles as well as particles inside grain bodies, and the resulting IGC is accompanied by slight pitting. When the heating temperature ex-

ceeds the eutectic temperature, non-equilibrium melting introduces severe IGC.

3. High corrosion susceptibility of microstructure in heat affected zone is related to both overageing during heating and the process of precipitation on grain boundaries during cooling.

## REFERENCES


[1] S. P. Ringer, K. Hono, Mater. Charact. **44**, 101 (2001).

[2] S. K. Son, M. Takeda, M. Mitome, Y. Bando, T. Endo, **59**, 629 (2005).

[3] S. Abis, M. Massazza, P. Mengucci, G. Riontino, Scripta Mater. **45**, 685 (2001).

[4] M. Wada, H. Kita, T. Mori, Acta Metall. **33**, 1631 (1985).

[5] Z. Liu, P. H. Chong, A. N. Butt, P. Skeldon, G. E. Thompson, Appl. Surf. Sci. **208/209**, 399 (2003).

[6] K. S. Rao, G. M. Reddy, K. P. Rao, Mater. Sci. Eng. A **403**, 69 (2005).

[7] L. B. Ber, Mater. Sci. Eng. **A280**, 83 (2000).

[8] P. Campestrini, E. P. M. van Westing, H. W. van Rooijen, J. H. W. de Wit, Corros. Sci. **42**, 1853 (2000).

[9] C. Blanc, B. Lavelle, G. Mankowski, Corros. Sci. **39**, 45 (1997).

[10] V. Guillaumin, G. Mankowski, Corros. Sci. **41**, 421 (1999).

[11] C. Blanc, A. Freulon, M. Ch. Lafont, Y. Kihn, G. Mankowska, Corros. Sci. **48**, 3838 (2006).

[12] T. Y. Liu, J. S. Robinson, M. A. McCarthy, J. Mater. Proc. Technol. **153-154**, 85 (2004).

[13] J. R. Galvele, S. M. de Micheli, Corros. Sci. **10**, 795 (1970).

[14] D. A. Little, B. J. Connoloy, J. R. Scully, Corros. Sci. **49**, 347 (2007).

[15] G. Svenninsen, M. H. Larsen, J. H. Nordlien, K. Nisanciogl, Corros. Sci. **48**, 58 (2006).

[16] R. P. Wei, C. M. Liao, M. Gao, Metall. Mater. Trans. A **29 A**, 1153 (1998).

[17] O. Reiso, H. G. Øverlie, N. Ryum, Metall. Trans. A **21A**, 1689 (1990).

[18] Y. S. Sato, S. H. C. Park, M. Michiuchi, H. Kokawa, Scri. Maters. **50**, 1233 (2004).


*Received: 20 June 2008.*